

# Development of Low-Heat-Capacity Pressure Roller

Akira Kato<sup>1</sup>, Yuuki Nishizawa<sup>1</sup>, Yasuo Yoda<sup>1</sup>, Jun Hara<sup>2</sup>, Hisashi Nakahara<sup>1</sup>, Takao Kikutani<sup>3</sup>, Masayuki Suekuni<sup>3</sup>, Toshihiko Ochiai<sup>4</sup>

<sup>1</sup> Peripherals Development Center 1, Canon Inc., Shizuoka, Japan

<sup>2</sup> Peripherals Development Center 2, Canon Inc., Kanagawa, Japan

<sup>3</sup> Simulation & Analysis R&D Center, Canon Inc., Tokyo, Japan

<sup>4</sup> Formerly of Canon Inc.

## Abstract

*In the quest to produce energy-saving laser beam printers, the most promising solution is a fuser unit with low heat capacity. However, the rise in temperature at the non-paper feeding region causes problems. Canon has developed a low-heat-capacity pressure roller that reduces the required warm-up power. The pressure roller has an elastic layer and an outer layer of PFA (polytetrafluoroethylene). The elastic layer is made of sponge silicone rubber containing thermally conductive filler. In this study, we conducted heat transfer simulations to examine the influence of the physical properties of heat in terms of saving energy and suppressing the temperature rise of the non-paper region. A low heat permeability coefficient reduced the required warm-up power, and high heat conduction effectively suppressed the temperature rise of the non-paper region.*

## Introduction

Reduction of power consumption in laser printers is an ongoing challenge. Canon presently uses an on-demand system that reduces the power needed during startup of the fuser.

To further reduce the startup power, fuser units with a smaller heat capacity need to be developed. However, the rise in temperature in the non-paper feeding region of the low-heat-capacity fuser poses a problem.

Canon has developed a low-heat-capacity pressure roller that combines both reduced startup power and control of the temperature rise in the non-paper region.

Thus, in this study, the impact of the thermal properties of the pressure roller in relation to reducing the startup power and controlling the temperature rise in non-paper regions was investigated using a heat transfer simulation for fusers.

## Low-Heat-Capacity Pressure Roller

A cross-sectional image of the newly developed low-heat-capacity pressure roller is shown in Fig. 1. This pressure roller is composed of PFA (polytetrafluoroethylene) as the surface layer, silicone rubber as the elastic layer, and an aluminum core.

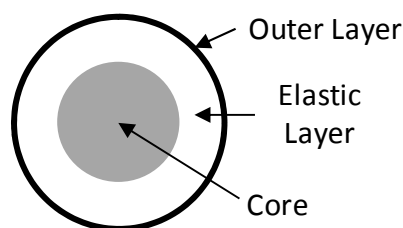


Fig. 1 Sectional image of pressure roller

Instead of using the conventional solid silicone rubber as the elastic layer, the low-heat-capacity pressure roller uses a sponge silicone rubber that contains thermally conductive filler.

An enlarged photo of the pressure roller is shown in Fig. 2. The conventional solid silicone rubber is shown in (a), and the sponge silicone rubber containing thermally conductive filler is shown in (b). It can be seen in Fig. 2(b) that the silicone rubber has pores.

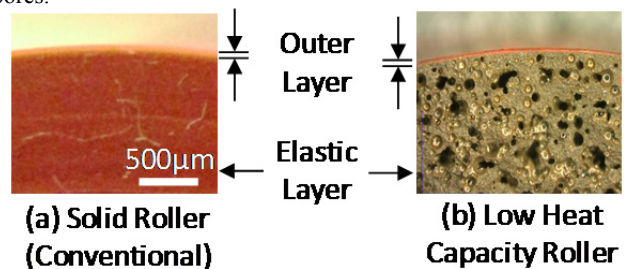


Fig. 2 Sectional photograph of pressure roller

Compared to traditional solid rubber pressure rollers, the low-heat-capacity pressure roller reduces the startup power by 10% with nearly the same rise in temperature at the non-paper regions. In this case, the thermal permeability was approximately three-quarters, and raising the thermal conductivity by approximately 20%.

## Performance Evaluation Using Heat Transfer Simulation

In this study, the impact of the thermal properties of the pressure roller in relation to reducing the startup power and controlling the temperature rise in non-paper regions was investigated using a heat transfer simulation for fuser units.

### Outline of heat transfer simulation

In the simulation, consideration was given to heat transfer inside the parts through heat conduction based on Fourier's law, as well as heat transfer to the air through convection based on Newton's law. In addition, the conductive thermal resistance for heat transfer between parts was also considered. [1]

Figure 3 shows a two-dimensional heat transfer simulation model for a fuser.

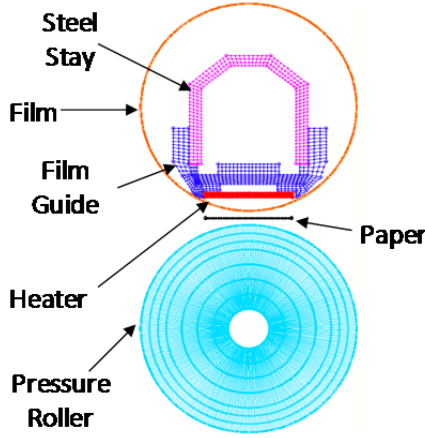


Fig. 3 Simulation model

A fuser with an on-demand system forms a fixing nip using PI (polyimide) substrate film and the pressure roller. Heat is supplied directly from the inner surface of the film to the fixing nip through the heater that is located inside the film. The heater is pressurized in the direction of the pressure roller based on the liquid crystal polymer film guide, the steel stay, and a pressure mechanism (which is not shown). In this process, the fixing nip is formed, and the paper that is fed to the fixing nip is heated and pressurized.

Table 1 Constitution of components

		Material	Thickness
Film	Base	PI	60 $\mu\text{m}$
	Top	PFA	10 $\mu\text{m}$
Heater	Base	$\text{Al}_2\text{O}_3$	1 mm
	Top	Glass	60 $\mu\text{m}$
Pressure Roller	Outer Layer	PFA	10 $\mu\text{m}$
	Elastic Layer	Silicone Rubber	3.5 mm
	Core	Aluminum	Diameter 13 mm

By simulating the heater, film, paper, pressure roller, film guide, and stay, thermal contact was established between the heater and film; film and pressure roller; film and paper; paper and pressure roller; heater and film guide; and film guide and stay. Furthermore, heat radiation to the air was also established from the outer circumference of the film and outer circumference of the pressure roller. The contact thermal resistance  $H$  ( $\text{mm}^2\text{K/W}$ ) based on actual measurements was applied between each of the components, and the heat loss coefficient  $R$  [ $\text{W/mm}^2\text{K}$ ] was applied to heat radiation.

The composition of the film, heater, and pressure roller used in the heat transfer simulation is shown in Table 1.

For the model calculations, 18 mm was used for the outer diameter of the film, 20 mm for the outer diameter of the pressure roller, and a width of 7 mm in the feeding direction for the heater. In addition, a temperature detection element (not shown) was attached to the back of the heater. As for other parameters, thermal conductivity  $\lambda$  [ $\text{W/mK}$ ], specific heat  $C_p$  [ $\text{J/kgK}$ ], density  $\rho$

[ $\text{kg/m}^3$ ], and initial temperature were applied to each component, and input power  $E$  [ $\text{W}$ ] was applied to the heater.

In the three-dimensional heat transfer simulation for the fuser, each of the fuser components described for the two-dimensional simulation was simulated in the vertical feeding direction.

As a fuser that feeds paper at the guide center in the paper width direction, in this analysis, the heat transfer simulation modeled halfway from the center of the feeding position.

### Comparison of startup power

Evaluation of the fuser startup power was carried out in the two-dimensional heat transfer simulation. First, calculations where constant power was input to the heater were made in a state where the film and pressure roller were rotating at a speed of 200 mm/s. The startup power of the fuser was evaluated based on the power  $E$  [ $\text{W}$ ] required for the temperature of the film surface (upstream side of fixing nip) to reach  $140^\circ\text{C}$  in three seconds.

The startup power was determined using the heat transfer simulation for the physical properties of the pressure roller elastic layer for the four conditions from (1) to (4) shown in Table 2.

Table 2 Heat physical properties of elastic layer

	$\lambda$ [W/mK]	$C_p$ [J/kgK]	$\rho$ [kg/m <sup>3</sup> ]	$P$ [J/m <sup>2</sup> s <sup>1/2</sup> K]
(1)	1.0	1500	1000	1225
(2)	0.5	1500	1000	866
(3)	0.5	1000	500	500
(4)	0.1	1000	500	224

With the required power  $E$  [ $\text{W}$ ] as the relative value  $E$  [a.u.], the startup power  $E$  [a.u.] in relation to the thermal permeability  $P$  [ $\text{J/m}^2\text{s}^{1/2}\text{K}$ ] of the pressure roller elastic layer is shown in Fig. 4.

Here, the thermal permeability  $P$  [ $\text{J/m}^2\text{s}^{1/2}\text{K}$ ] is given by:

$$P = \sqrt{\lambda \times C_p \times \rho}$$

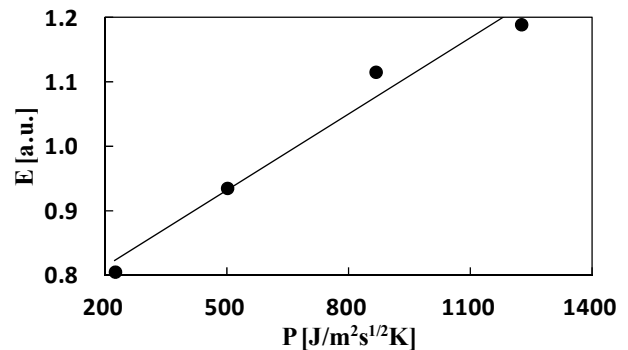


Fig. 4 Relationship between heat permeability coefficient and electricity

A correlation was found between the thermal permeability  $P$  [ $\text{J/m}^2\text{s}^{1/2}\text{K}$ ] and startup power  $E$  [a.u.], and by lowering the thermal permeability from 700 to 500  $\text{J/m}^2\text{s}^{1/2}\text{K}$ , it was possible to reduce the startup power by approximately 10%.

### Comparison of temperature rise in non-paper regions

Evaluation of the temperature rise in non-paper regions was carried out using three-dimensional heat transfer simulation. First, power was input to the heater in a state where the film and pressure roller were rotating at a speed of 200 mm/s. Paper feeding was started three seconds after power was input. The power input to the heater was controlled so that the temperature detected by the attached detection element reached 220°C.

For the paper, COM10 envelopes (width of 104.8 mm, length of 241.3 mm) Mailwell No. 582 were used. An interval of 100 mm (0.5 s) was set between each envelope, and 10 envelopes were continuously fed. The evaluation target was the temperature  $\Delta T$  [°C] at the location where there was the largest difference in temperature between the non-paper region at the upstream side of the pressure roller fixing nip and the paper-pass region.

A temperature contour diagram of the results of the three-dimensional heat transfer simulation is shown in Fig. 5.

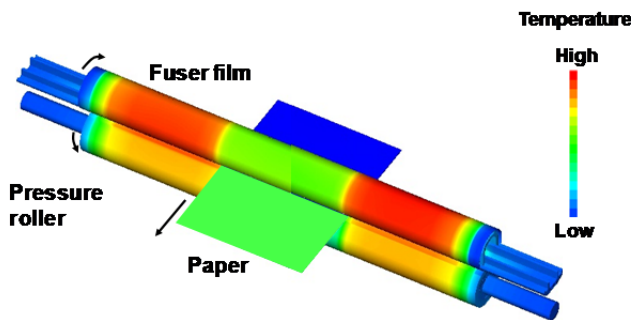


Fig. 5 Three-dimensional simulation

The temperature at the non-paper regions of the pressure roller  $\Delta T$  [°C] in relation to the thermal conductivity  $\lambda$  [W/mK] of the elastic layer of the pressure roller is shown in Fig. 6.

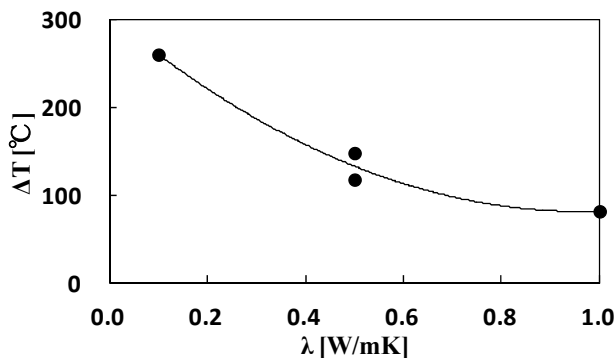


Fig. 6 Relationship between heat conductivity and temperature of non-paper feeding region

A correlation was found between the thermal conductivity  $\lambda$  [W/mK] and the temperature at the non-paper regions of the pressure roller  $\Delta T$  [°C], and by raising the thermal conductivity of the elastic layer from 0.1 to 1.0 W/mK, it was possible to reduce the temperature at the non-paper regions by approximately 180°C.

### Performance Evaluation Using Actual Equipment

Pressure rollers with different physical properties of the elastic layer were produced experimentally, and it was confirmed that the correlation between the physical properties predicted in the abovementioned simulation and the fuser performance is expressed even in the performance evaluation of the actual equipment.

Table 3 shows the thermal properties of the elastic layer of the experimentally produced pressure rollers. Item (5) represents the conventional solid silicone rubber, (6) the sponge silicone rubber containing thermally conductive filler, and (7) the sponge silicone rubber.

Table 3 Heat physical properties of elastic layer

	$\lambda$ [W/mK]	$C_p$ [J/kgK]	$\rho$ [kg/m <sup>3</sup> ]	$P$ [J/m <sup>2</sup> s <sup>1/2</sup> K]
(5)	0.16	1780	950	520
(6)	0.20	1350	750	450
(7)	0.17	1415	610	384

The power  $E$  [W] required for the film surface temperature (upstream side of fixing nip) to reach 140°C in three seconds, and the temperature in the non-paper regions of the pressure roller  $\Delta T$  [°C] when 10 envelopes are continuously fed were evaluated.

The startup power  $E$  [a.u.] in relation to the thermal permeability  $P$  [J/m<sup>2</sup>s<sup>1/2</sup>K] is shown in Fig. 7.

Actual measured values indicated by × are added for comparison with the simulation values indicated by ● in Fig. 4.

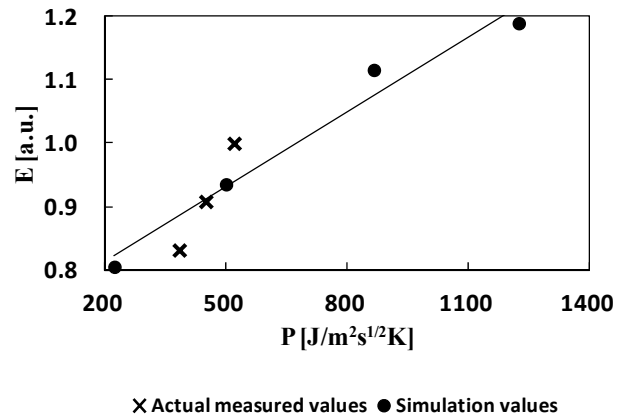


Fig. 7 Relationship between heat permeability coefficient and electricity

The actual measured values nearly matched the simulation plot; when the thermal permeability  $P$  of the elastic layer is lower, the power  $E$  is smaller.

Thus, the low-heat-capacity pressure roller reduced the startup power  $E$  [W] by approximately 10% compared to the traditional solid pressure roller.

Next, the temperature in the non-paper regions  $\Delta T$  [°C] in relation to the thermal conductivity  $\lambda$  [W/mK] is shown in Fig. 8.

Actual measured values indicated by  $\times$  are added for comparison with the simulation values indicated by  $\bullet$  in Fig. 6.

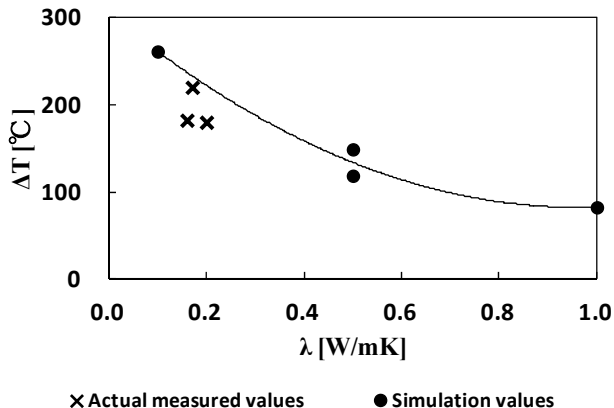


Fig. 8 Relationship between heat conductivity and temperature of non-paper feeding region

The actual measured values nearly matched the simulation plot; when the thermal conductivity  $\lambda$  of the elastic layer is higher, the temperature at the non-paper regions  $\Delta T$  is lower.

Thus, the temperature at the non-paper regions of the low-heat-capacity roller was able to be controlled to the same temperature as that of traditional solid pressure rollers.

It was confirmed that the correlation between the physical properties based on the simulation and the fuser performance is expressed even in the actual equipment.

## Conclusion

An analysis based on heat transfer simulations clarified that lowering the thermal permeability of the elastic layer of the pressure roller effectively reduced the startup power of the fuser, and increasing the thermal conductivity of the elastic layer of the pressure roller effectively controlled the temperature rise in the non-paper regions.

Based on these findings, we have developed a low-heat-capacity pressure roller that reduces the startup power and controls the temperature rise in non-paper regions.

Compared to traditional rollers, low-heat-capacity pressure rollers suppress the temperature rise in non-paper regions to the same level as that of traditional rollers, and also reduce the startup power by approximately 10%.

## References

- [1] Y. Otsuka, T. Ochiai, T. Sano, and Y. Nishizawa: Optimum Heater Designing for Low Energy Consumption Fuser, Pan-Pacific Imaging Conference 2008 (Tokyo, Japan), 196-199 (2008).

## Author Biography

Akira Kato received his B.E. degree in Applied Physics from Fukui University, Japan in 1996. He joined Canon Inc. in 1996 and has been engaged in the development of electrophotography.